2019 16th International Conference on Electrical Engineering, Computing Science and Automatic Control (CCE) Mexico City, Mexico.
September 11-13, 2019

Proposal of a speed sensor based on FGMOS for a MEMS rotatory micromotor

Luis Sánchez-Márquez
Electrical Engineering Dept.
CINVESTAV-IPN
Mexico City, Mexico
luis.sanchez.m@cinvestav.mx

Mario Alfredo Reyes-Barranca
Electrical Engineering Dept.
CINVESTAV-IPN
Mexico City, Mexico
mreyes@cinvestav.mx

Griselda Stephany Abarca-Jiménez
UNIDAD PROFESIONAL INTERDISCIPLINARIA CAMPUS HIDALGO INSTITUTO POLITÉCNICO NACIONAL
Hidalgo, 42162, Mexico
gabarcaj@ipn.mx

Andrea López-Tapia
Electrical Engineering Dept.
CINVESTAV-IPN
Mexico City, Mexico
andrea.lopez@cinvestav.mx

Luis Martín Flores-Nava
Electrical Engineering Dept.
CINVESTAV-IPN
Mexico City, Mexico
lmflores@cinvestav.mx

Oliverio Arellano-Cárdenas
Electrical Engineering Dept.
CINVESTAV-IPN
Mexico City, Mexico
arellano@cinvestav.mx

***Abstract*—This paper shows a proposal design of how to use a Floating-gate MOS transistor (FGMOS) for estimation of the rotational speed of a MEMS rotatory micromotor. The design is based on the 0.5 micron CMOS technology. With simulations carried out in SPICE, it is shown how the change in the capacitance between the control gate and the floating gate can be used to estimate the rotational speed of a micromotor.**

Keywords— FGMOS, micromotor, turning speed.

I. INTRODUCTION

Within the diverse applications of the floating-gate metal oxide semiconductor transistor (FGMOS), there is the one to use it as a transducer of mechanical to electrical signals [1]. This work proposes a structure for an FGMOS that will allow to estimate the turning speed of a MEMS (micro electro mechanic system) rotatory micromotor. The motor is designed with the rules available from the 0.5 micron CMOS technology of On Semiconductor [2].

Micromotors manufactured using CMOS technology or technologies dedicated to the manufacture of MEMS, such as MEMSCAP [3], are reported in [4] [5] [6]. These designs do not integrate the structures of the micromotor and a speed sensor on one chip. The present work shows a proposal to achieve it.

A. FGMOS review

The structure of an FGMOS is shown in Fig. 1. This transistor consists of the bulk (B), the drain (D), the source (S), two gates: a floating gate (FG) and a control gate located above FG. The FG is electrically isolated.

The capacitances equivalent circuit of the FGMOS is shown in Fig. 2, where the sensing capacitance (*Cc*) is the capacitance formed by the control gate and the floating gate; *CD* is the parasitic capacitance due to the overlap between FG and D; *CS* is the parasitic capacitance due to the overlap between FG and S; *COX* is the capacitance between FG and B.

If the circuit of Fig. 3(a) is connected, the equivalent is as the one shown in Fig. 3(b).

The floating gate voltage (V_{FG}) is obtained by performing the circuit analysis and it is given by:

$$V_{FG}=\frac{Cc}{C_{TOT}}V_o+\frac{CD}{C_{TOT}}V_{DS} \tag{1}$$

Where

$$C_{TOT}=Cc+CD+CS+COX \tag{2}$$

Normally *CD* is much smaller than C_{TOT} [7], so V_{FG} can be approximated as follows:

$$V_{FG}\approx\frac{Cc}{C_{TOT}}V_o=K_{CG}V_o \tag{3}$$

Where K_{CG} is known as the coupling coefficient, whose value is always <1. Consequently, V_{FG} will be a fraction of V_o.

The drain current of a N-channel FGMOS in the saturation regime is given by:

$$I_D=\frac{\beta}{2}(V_{FG}-V_{TH})^2=\frac{\beta}{2}\left(\frac{Cc}{C_{TOT}}V_o-V_{TH}\right)^2 \tag{4}$$

Where V_{TH} is the threshold voltage of the transistor and β is known as transconductance parameter [8] and is given by:

978-1-7281-4840-3/19/$31.00 ©2019 IEEE

$$\beta=\mu_n \frac{\varepsilon_{ox}}{t_{ox}} \frac{W}{L} \quad (5)$$

Where μ_n is the mobility of the electrons; ε_{ox} is the SiO_2 dielectric constant; t_{ox} is the thickness of the oxide; W is the channel width and L is the channel length.

From (4) it can be seen that if the sensing capacitance (Cc) varies, it is possible to modify the floating gate voltage, which in turn will cause the drain current to change. This fact can be used in the design of the structure for the measurement of the micromotor rotation speed.

B. *Micromotors review*

Micromotors are devices that generate a movement due to some micro-acting force. The actuation forces for micromotors are primarily electrostatic forces. The force generated in parallel pairs of misaligned and electrically energized plates stimulates the movement required in a micromotor [9].

There are two types of micromotors: lineal motors and rotatory motors [9].

Fig. 4 shows a rotatory micromotor, whose rotor (formed by a single piece) and stator are made of a conductive material. The stator poles are connected in an alternating sequence of three electrical phases (φ_1 is connected to E1, φ_2 is connected to E2 and φ_3 is connected to E3). If a potential difference (control voltage) with a specific minimum value is applied to the misaligned poles, an electrostatic force between them is generated. This force causes the rotor to rotate one step; if this is done in an appropriate sequence and periodically, the rotor rotates at a certain speed in a clockwise or counterclockwise direction [9]. By the way they turn, these engines are also called stepper motors.

It is worth to mention that there are technologies dedicated to the manufacture of MEMS micromotors, such as MEMSCAP [3], however, it is also possible to manufacture them using CMOS-MEMS technology. These designs must comply with their particular CMOS technology design rules, e.g. those of On Semiconductor [2]. This approach implies that after their fabrication a surface micromachining post-process must be carried out [4].

II. Structure of the Proposed FGMOS-Based Velocity Estimation System

The proposed structure of the sensor is intended to be used to measure the rotational speed of a rotary micromotor. This motor is designed following the rules of the 0.5 micron CMOS technology of On Semiconductor [2]. The rotor is built with the Metal2 layer (Aluminum) available in this technology.

Fig. 5 shows a schematic of how the floating-gate MOS transistor is built. Fig. 5 (a) shows a capacitor: the upper plate (control gate) is made with the Metal1 layer [2] and the lower plate (floating gate) is built with the Poly1 layer [2]. Fig. 5 (b) shows metal contacts (Via1 [2]) distributed throughout the entire CG plate; notice that this figure is only illustrative for a better understanding of the reader, since in the real process when the Metal2 is deposited, the Via1 layer is also deposited. Fig. 5 (c) shows the CG plate fixed to the rotor structure (made with Metal2) by means of the metal contacts. Finally, the gate of a transistor (made with the Poly1 layer) extends to the non-moving plate FG.

The proposed shape of the sensing capacitor plates is that of a semi-ring (Fig. 6). The radiuses r_1 and r_2 of the geometry are of a magnitude such that Cc does not interfere with the rotation of the rotor.

The definition of the angles θ_f y θ_c must ensure that, over the entire course of the rotor rotation, there is always an overlap of the plates (see Fig. 7).

A. *Electrical connections of the FGMOS*

Since the control gate (CG) is connected by means of metal contacts to the micromotor rotor, if the rotor is connected to the positive potential of the control voltage (V_o), the control gate is also connected to the same potential. Fig. 8 shows the electrical connections of the FGMOS; the arrow in the gates FG and CG indicates that the capacitance Cc is variable.

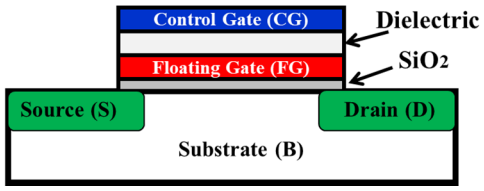

Fig. 1. Schematic of the cross section of an FGMOS

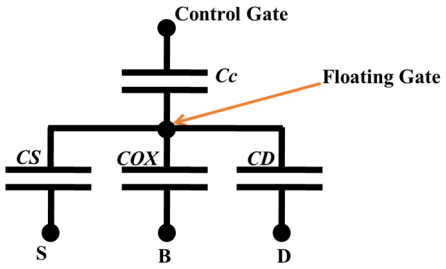

Fig. 2. Simplified equivalent circuit of the capacitances of an FGMOS

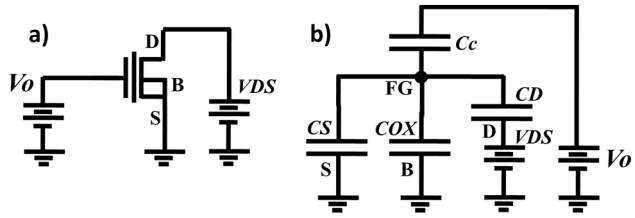

Fig. 3. (a) FGMOS connected to a voltage source *VDS* in the drain and *Vo* in the control gate (b) Equivalent circuit

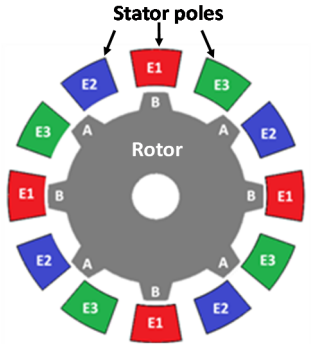

Fig. 4. Schematic of a rotatory micromotor

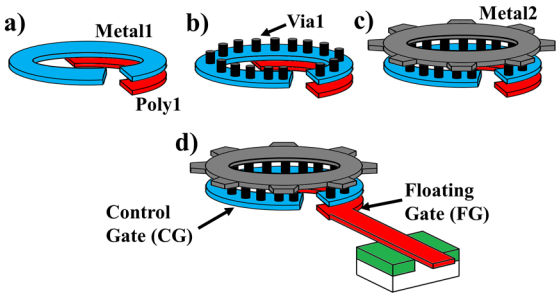

Fig. 5. (a) Capacitor *Cc* (b) Metal contacts on the CG plate (c) The rotor (Metal2) is fixed to the CG plate by means of metal contacts. (d) The FG plate extends and forms the floating gate of the FGMOS

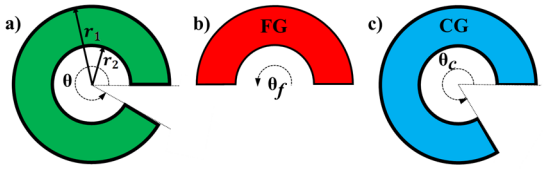

Fig. 6. (a) Semi-ring (b) FG plate formed with Poly1 (c) CG plate formed with Metal1

B. *Sensing capacitance variation*

If the rotor rotates, the overlap between plates CG and FG varies. This causes the capacitance *Cc* to changes as shown in Fig. 9 (b).

The maximum capacitance is obtained when the maximum overlap of plates CG and FG occurs (between points A and B of Fig. 9(b)) and its value is given by:

$$Cc_{max}=\frac{A_{max}\varepsilon_{air}}{d_{cc}}=\frac{\frac{\theta_{max}}{2}\left(r_1^2-r_2^2\right)*\varepsilon_{air}}{d_{cc}} \quad (6)$$

Where d_{cc} is the separation between plates FG and CG; θ_{max} is the maximum overlapping angle and ε_{air} is the air dielectric constant.

The minimum capacitance is obtained when the minimum overlap of plates CG and FG occurs (between points C and D of Fig. 9(b)) and its value is given by:

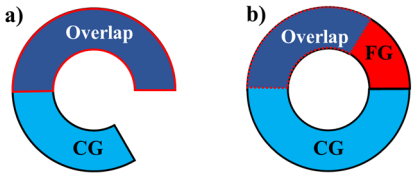

Fig. 7. Sensing capacitor (*Cc*) (a) The CG and FG plates in a maximum overlap (b) The CG and FG plates in a minimum overlap

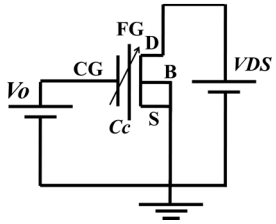

Fig. 8. Schematic circuit of the FGMOS electrical connections

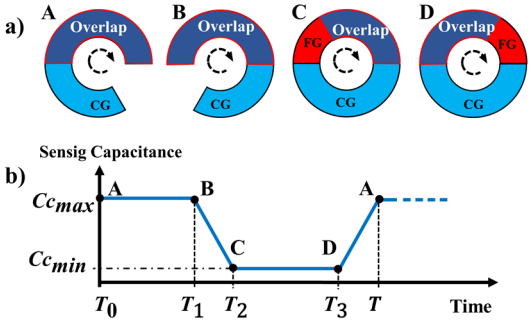

Fig. 9. (a) Rotor rotating in the clockwise direction (b) Behavior of sensing capacitance when the rotor turns

$$Cc_{min}=\frac{A_{min}\varepsilon_{air}}{d_{cc}}=\frac{\frac{\theta_{min}}{2}\left(r_1^2-r_2^2\right)*\varepsilon_{air}}{d_{cc}} \quad (7)$$

Where θ_{min} is the minimum overlapping angle.

The sensing capacitance changes with each rotor step (decreases between points B and C and increases between D and A of Fig. 9) and this change is given by:

$$Cc_{step}=\frac{A_{step}\varepsilon_{air}}{d_{cc}} \quad (8)$$

Where A_{step} is the overlap area that increases or decreases with each motor step and is given by:

$$A_{step}=\frac{\theta_{step}}{2}*\left(r_1^2-r_2^2\right) \quad (9)$$

θ_{step} is the angular displacement that occurs when the rotor rotates one step.

C. *Variation of the coupling coefficient K_{CG}*

For this FGMOS structure, there is a parasitic capacitance (C_{poly}) between the FG plate (built with Poly1) and the bulk, so (2) changes to:

$$C_{TOT}=Cc+CD+CS+COX+C_{poly} \quad (10)$$

Where

$$C_{poly}=\frac{\varepsilon_{ox}A_{poly}}{d_{P1B}} \quad (11)$$

A_{poly} is the FG plate area and is given by:

$$A_{poly}=\frac{\theta_f}{2}*\left(r_1^2-r_2^2\right) \quad (12)$$

And d_{P1B} is the distance between the Poly1 layer and the bulk [2].

Normally the values of *CD*, *CS* and *COX* are very small compared to C_{poly}. So K_{CG} can be approximated as:

$$K_{CG}\approx\frac{Cc}{Cc+C_{poly}} \quad (13)$$

That is, K_{CG} is modified with the variation of *Cc*, in such a way that K_{CG} would be expected to have a behavior as shown in Fig. 10.

Where

$$K_{CG\,max}\approx\frac{Cc_{max}}{Cc_{max}+C_{poly}} \quad (14)$$

$$K_{CG\,min}\approx\frac{Cc_{min}}{Cc_{min}+C_{poly}} \quad (15)$$

D. *Calculation of the rotor turning speed.*

In (3) and (4) it is observed that when K_{CG} increases, the drain current also increases, so that when the rotor rotates, the current should have a behavior similar to that shown in Fig. 11 (b).

If the rotor rotates at a constant speed, the time that takes the structure to take a turn is measured (by measuring the period T of the signal at the output of the FGMOS) and the angular velocity of the rotor (given in radians per second) is calculated as follows:

$$\omega_{rotor}=\frac{2\pi}{T} \quad (16)$$

Or in revolutions per minute:

$$v_{rpm}=\frac{30}{\pi}\omega_{rotor}=\frac{60}{T} \quad (17)$$

III. Results

A. *Parametric analysis in SPICE*

Using the following parameters for the FGMOS structure: θ_f=180° ; θ_c=300° ; r_1=200 µm ; r_2=180 µm ; *W*=1.2 µm ; *L*=0.9µm ; d_{cc}=0.388 µm and a control voltage V_0=18V , a simulation in SPICE was performed in order to know how the drain current changes when the sensing capacitance value (*Cc*) is modified. The simulated circuit is shown in Fig. 8.

The rotor's rotation is emulated (twelve steps) by setting *Cc* as a parameter. The minimum capacitance due to the overlap of CG and FG is 0.1819 pF and the maximum capacitance is 0.27286 pF, with steps of 7.58fF. Fig. 12 shows the FGMOS output characteristics plot for all the thirteen values of *Cc*. It is observed that the drain current increases when the sensing capacitance grows.

A value of *VDS*=5V is selected and the behavior of the coupling coefficient (K_{CG}), the control gate voltage (V_{FG}) and the drain current (I_D) are plotted for the thirteen values of the sensing capacitance.

Fig. 13 shows these results. It is observed that the coupling coefficient, the control gate voltage and the drain current have a linear behavior with the changes in the sensing capacitance.

From Fig. 13 (b) it is obtained that the maximum floating gate voltage is $V_{FG\,max}$=3.7V and the maximum sensing capacitor voltage is $V_{CC\,max}=V_o-2.65$V=15.35V.

The gate oxide breakdown voltage for the 0.5 micron CMOS technology is V_{Box}=9.87V [7]. This value is greater than $V_{FG\,max}$, therefore there is no risk of oxide breakdown.

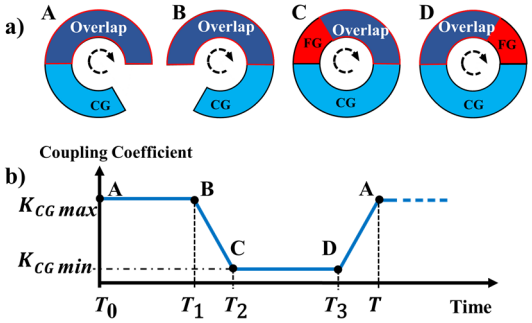

Fig. 10. (a) Rotor rotating in the clockwise direction (b) Behavior of the coupling coefficient when the rotor rotates

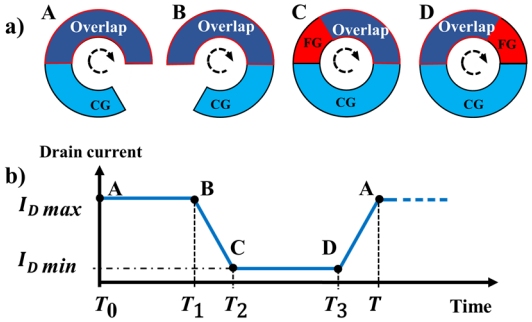

Fig. 11. (a) Rotor rotating in the clockwise direction (b) Behavior of the drain current when the rotor rotates

When the distance between two electrodes is less than one micron, the maximum electric field in air environment is $350\text{x}10^6$ V/m [10]. With d_{cc}=0.388 µm, the sensing capacitor breakdown voltage is $V_{B_{CC}}$=135.8 V . i.e. $V_{CC\,max}<V_{B_{CC}}$, therefore there is no risk of breakdown.

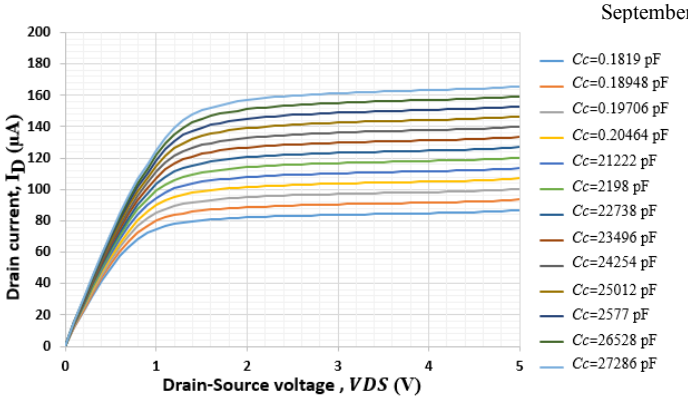

Fig. 12. FGMOS output characteristic plot

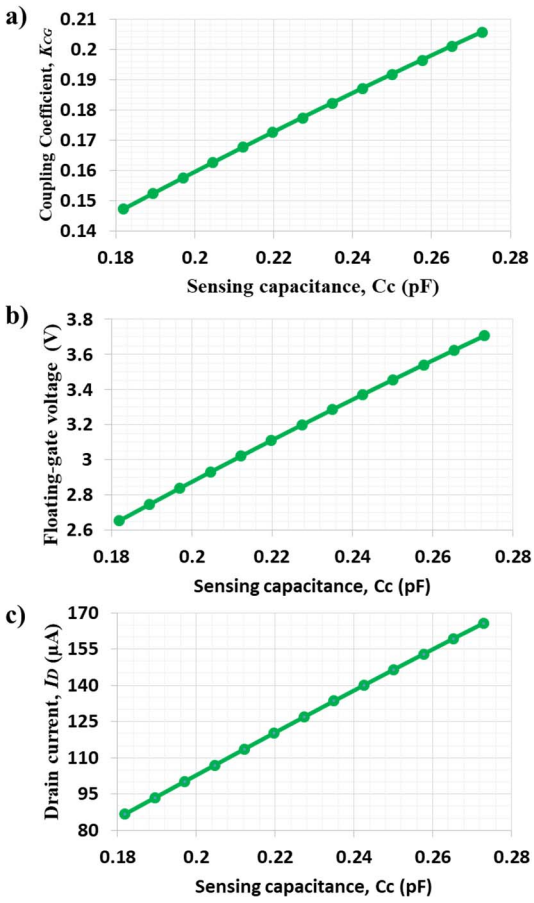

Fig. 13. (a) Coupling coefficient against sensing capacitance (b) Floating gate voltage against sensing capacitance (c) Drain current against sensing capacitance.

B. *Transient analysis in SPICE*

Finally, a transient analysis of the drain current is performed.

Because in SPICE it is not possible to simulate a capacitor that varies with time [7], the simulation was performed by making the variations in the floating gate voltage. This is possible since as it was observed in Fig. 13(b), V_{FG} changes linearly with Cc. The circuit used for this simulation is that shown in Fig. 14(a). The voltage supply generates the signal of Fig. 14(b), emulating that the rotor is taking one step per millisecond. With this, the drain current behaves as shown in Fig. 14(c).

The calculation of the turning speed is simply obtained using (16) and (17).

$$\omega_{rotor}=83.77\frac{\text{rad}}{\text{s}}$$

Or in revolutions per minute:

$$v_{rpm}=800\text{ rpm}$$

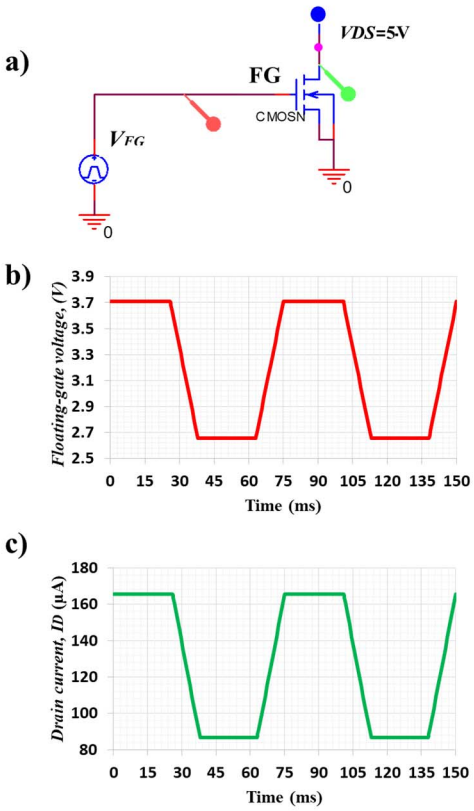

Fig. 14. Drain current transient analysis (a) Schematic circuit (b) Signal on the floating gate (c) Drain current.

IV. Conclusions

It is possible to use a floating-gate transistor (FGMOS) as the main element to measure the turning speed of a rotatory micromotor based on CMOS-MEMS technology. Considering the design rules of the 0.5 micron CMOS technology of On Semiconductor, semi-ring type structures were proposed as control gate and floating gate. It was observed that when the sensing capacitance varies, a linear change is observed in the coupling coefficient and in the floating gate voltage. This allow having a linear variation in drain current (with values between 87 µA and 165 µA) and it can be correlated with the rotational speed of the micromotor.

REFERENCES

[1] G. S. Abarca-Jiménez and M. A. Reyes-Barranca, MEMS capacitive sensor using FGMOS, Mexico City: 10th International Conference on Electrical Engineering, Computing Science and Automatic Control (CCE), 2013.

[2] OnSemiconductor, C5X, 0.5 Micron Technology Design Rules, 2011.

[3] MEMSCAP, 2011-2012. [Online]. Available: http://www.memscap.com/products/mumps/polymumps.

[4] J. Horstmann and K. Goser, Monolithic integration of a silicon micromotor in combination with the CMOS drive circuit on one chip, Germany, 2003.

[5] Dhananjay Barbade, Rohit Soni and Shriniwas Metan, Micromotor Fabrication by Surface Micromachining Technique, India, 2010.

[6] M. A. Basha, S. Safavi-Naeini and S. K. Chaudhuri, Design and fabrication of an electrostatic micromotor with a low operating voltage, Canada, 2007.

[7] L. Sánchez-Márquez, Diseño y análisis de un micromotor angular basado en tecnología CMOS-MEMS, Mexico City, 2018.

[8] R. J. Baker, CMOS Circuit Design, Layout, and Simulation, New York: IEEE PRESS, 1998.

[9] H. Tai-Ran, MEMS and microsystems : design and manufacture, McGraw-Hill, 2002.

[10] A. Peschot, C. Poulain, N. Bonifaci y O. Lesaint, Electrical Breakdown Voltage in Micro- and Submicrometer Contact Gaps (100nm - 10μm) in Air and Nitrogen, California, Berkeley, 2015.